

indeed represent traces of crown-group metazoans. The evidence is currently insufficient to decide between the three.

The Stirling biota offers a glimpse of a biosphere >1200 million years ago, which was more complex than the singularly microbial-algal world that is usually assumed. If our interpretation of the biota is correct, there is a challenge for paleontologists and geobiologists to find plausible mechanisms that prevented a biosphere evidently containing large motile organisms from erupting into Phanerozoic-type diversity until >600 million years later, during the Cambrian explosion. Extreme environmental conditions during the late Neoproterozoic (34) may have been the final bottleneck before which no diversification of organisms with metazoan-like modes of life could have had lasting success.

References and Notes

1. J. W. Valentine, D. Jablonski, D. H. Erwin, *Development* **126**, 851 (1999).
2. G. E. Budd, S. Jensen, *Biol. Rev. Camb. Philos. Soc.* **75**, 253 (2000).
3. S. Conway Morris, *Proc. Natl. Acad. Sci. U.S.A.* **97**, 4426 (2000).
4. A. Seilacher, P. K. Bose, F. Pflüger, *Science* **282**, 80 (1998).
5. P. Cloud, *Geology* **1**, 123 (1973).
6. G. A. Wray, J. S. Levinton, L. H. Shapiro, *Science* **274**, 568 (1996).
7. L. Bromham, A. Rambaut, R. Fortey, A. Cooper, D. Penny, *Proc. Natl. Acad. Sci. U.S.A.* **95**, 12386 (1998).
8. F. J. Ayala, A. Rzhetsky, F. J. Ayala, *Proc. Natl. Acad. Sci. U.S.A.* **95**, 606 (1998).
9. A. Cooper, R. A. Fortey, *Trends Ecol. Evol.* **13**, 151 (1998).
10. P. C. Muhling, A. T. Brakel, *Mount Barker-Albany, WA, 1:250,000 Geological Series Explanatory Notes* (Geological Survey of Western Australia, Perth, 1985).
11. J. S. Myers, in *Geology and Mineral Resources of Western Australia* (Geological Survey of Western Australia, Perth, 1990), pp. 255–264.
12. J. Beeson, thesis, University of Western Australia, Crawley (1991).
13. C. A. Boulter, *J. Struct. Geol.* **1**, 207 (1979).
14. T. Cruse, thesis, University of Western Australia, Crawley (1991).
15. ———, L. B. Harris, *Precambrian Res.* **67**, 1 (1994).
16. ———, L. B. Harris, B. Rasmussen, *Aust. J. Earth Sci.* **40**, 293 (1993).
17. A. Turek, N. C. N. Stephenson, *J. Geol. Soc. Aust.* **13**, 449 (1966).
18. Specimens were found by B.R. and are referred to as cf. *Palaeobullia* in (14), pp. 42 and 45.
19. J. G. Gehling, G. M. Narbonne, M. M. Anderson, *Palaeontology* **43**, 427 (2000).
20. R. Bromley, *Trace Fossils* (Chapman & Hall, London, ed. 2, 1996).
21. A. G. Collins, J. H. Lipps, J. W. Valentine, *Paleobiology* **26**, 47 (2000).
22. H. Kitazato, *J. Foram. Res.* **18**, 344 (1988).
23. O. Rauprich et al., *J. Bacteriol.* **178**, 6525 (1996).
24. M. F. Glaessner, *Lethaia* **2**, 369 (1969).
25. Supplementary notes, including details of the geochronological procedures, SHRIMP U-Pb data for detrital zircon, and SHRIMP U-Pb data for monazite cores and overgrowths, are available on Science Online at www.sciencemag.org/cgi/content/full/296/5570/1112/DC1.
26. J. A. Evans, J. A. Zalasiewicz, *Earth Planet. Sci. Lett.* **144**, 421 (1996).
27. B. Rasmussen, I. R. Fletcher, N. J. McNaughton, *Geology* **29**, 963 (2001).
28. G. Foster, P. Kinny, D. Vance, C. Prince, N. Harris, *Earth Planet. Sci. Lett.* **181**, 327 (2000).
29. J. B. Smith et al., *Precambrian Res.* **88**, 143 (1998).

30. G. C. Dawson, B. Krapez, I. R. Fletcher, N. J. McNaughton, B. Rasmussen, in preparation.
31. L. P. Black, L. B. Harris, C. P. Delor, *Precambrian Res.* **59**, 117 (1992).
32. L. B. Harris, *J. Geol. Soc. London* **151**, 901 (1994).
33. A. G. Collins, *Proc. Natl. Acad. Sci. U.S.A.* **95**, 15458 (1998).
34. P. F. Hoffman, A. J. Kaufman, G. P. Halverson, D. P. Schrag, *Science* **281**, 1342 (1998).
35. We thank R. Bromley, T. Cruse, D. Grazhdankin, S. Jensen, J. Lipps, S. Revets, B. Runnegar, A. Seilacher, S. Sheppard, O. Tendal, and M. Whitehouse for comments and discussion and B. David, W. Kempff, A. Kennedy, P. Kinny, B. Krapez, M. Marshall, and staff members of the University of Western Aus-

tralia's Centre for Microscopy and Microanalysis for assistance. Manuscript drafts were critically reviewed by S. Jensen, B. Runnegar, and A. Seilacher. This work was supported by an Australian Research Council (ARC) fellowship and grant to B.R. Samples were collected with the permission of the Western Australian Department of Conservation and Land Management. Zircon and monazite grains were analyzed with SHRIMP II, operated by a consortium consisting of Curtin University of Technology, the Geological Survey of Western Australia, and the University of Western Australia, with ARC support.

23 January 2002; accepted 26 March 2002

Female Germ Cell Aneuploidy and Embryo Death in Mice Lacking the Meiosis-Specific Protein SCP3

Li Yuan, Jian-Guo Liu, Mary-Rose Hoja, Johannes Wilbertz, Katarina Nordqvist,* Christer Höög†

Aneuploidy (trisomy or monosomy) is the leading genetic cause of pregnancy loss in humans and results from errors in meiotic chromosome segregation. Here, we show that the absence of synaptonemal complex protein 3 (SCP3) promotes aneuploidy in murine oocytes by inducing defective meiotic chromosome segregation. The abnormal oocyte karyotype is inherited by embryos, which die in utero at an early stage of development. In addition, embryo death in SCP3-deficient females increases with advancing maternal age. We found that SCP3 is required for chiasmata formation and for the structural integrity of meiotic chromosomes, suggesting that altered chromosomal structure triggers non-disjunction. SCP3 is thus linked to inherited aneuploidy in female germ cells and provides a model system for studying age-dependent degeneration in oocytes.

Aneuploidy is the leading known cause of pregnancy loss and has been recorded in ~25% of all conceptions and 0.3% of all newborns (1). Aneuploidy in germ cells is predominantly due to aberrant female meiotic chromosome segregation, where increasing maternal age represents a well-documented risk factor. Homologous chromosomes (homologs) in meiotic cells undergo pairing (called synapsis) and recombination during which physical links, chiasmata, are established between them. Synapsis is aided by a meiosis-specific protein complex, the synaptonemal complex (SC), which comprises two axial lateral elements (AEs) and a central element (CE) (2). The two AEs, which colocalize with the sister chromatids of each homolog, become connected along their entire

length by fine fibers called transversal filaments (TFs) at the pachytene stage of meiotic prophase I (3). The AE is composed of discrete protein filaments, organized by the cohesin complex (4) or by two meiosis-specific proteins, synaptonemal complex protein 2 (SCP2) and SCP3 (5). SCP3 is required for AE formation and for male fertility (6–8). The function of SCP3 during the meiotic cell divisions is unclear, however, because SCP3^{-/-} male germ cells die around the zygotene stage of meiosis (8).

Here, we analyze the functional role(s) of SCP3 in meiotic chromosome segregation in female germ cells. Twelve-week-old wild-type and SCP3-deficient females were mated with wild-type males. In contrast to SCP3-deficient males, SCP3-deficient females were fertile and generated healthy offspring (Fig. 1A). However, the SCP3-deficient females exhibited a sharp reduction in litter size, generating on average 5.9 offspring per female, compared with 8.9 offspring for their wild-type siblings (Fig. 1A). This reduction could be due to ovarian failures, resulting in functional oocyte loss. A comparison of ovarian morphology in SCP3-

Center for Genomics and Bioinformatics and Department of Cell and Molecular Biology, Karolinska Institutet, SE-171 77 Stockholm, Sweden.

*Present address: Molecular Sciences, Astra Zeneca R&D, SE-151 85 Södertälje, Sweden.

†To whom correspondence should be addressed. E-mail: christer.hoog@cmb.ki.se

REPORTS

deficient and wild-type females indicated, however, that follicular development is not affected in *SCP3*-deficient females (9). To investigate the possibility of embryonic death in utero, *SCP3*-deficient or wild-type females (12 weeks of age) were mated with wild-type males. An embryo count at 11.5 days post coitum (dpc)

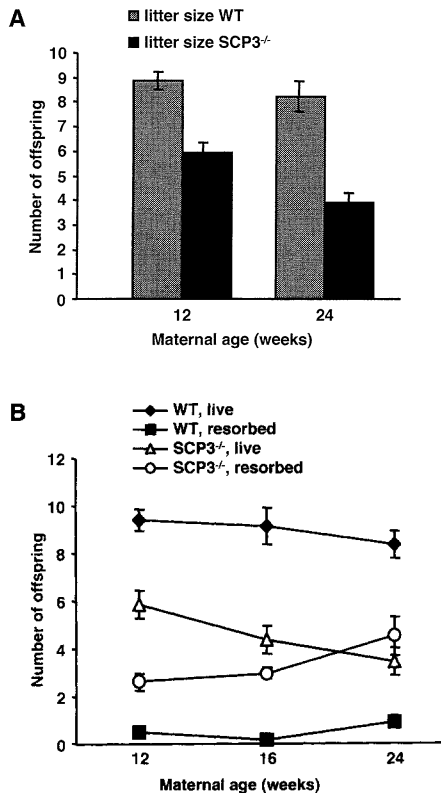


Fig. 1. Absence of *SCP3* affects embryo survival. **(A)** 12- and 24-week-old wild-type and *SCP3*-deficient females were mated with wild-type males and the number of pups born counted (13). Twenty-eight wild-type and 26 *SCP3*-deficient 12-week-old female, as well as 15 wild-type and *SCP3*-deficient 24-week-old females, respectively, were used in these studies. *SCP3*-deficient females generated significantly fewer offspring compared to wild-type females of the same age ($P < 0.001$, Student's two-tailed t -test). Furthermore, 24-week-old *SCP3*-deficient females produced significantly fewer offspring than 12-week-old *SCP3*-deficient females ($P < 0.05$, Student's two-tailed t -test). **(B)** 12-, 16-, and 24-week-old *SCP3*-deficient and wild-type female siblings were mated with wild-type males. Seventeen, 11, and 16 wild-type and 16, 12, and 16 *SCP3*-deficient females were used for each respective age group. Pregnant females were sacrificed at 11.5 dpc (13). *SCP3*-deficient females had significant embryo resorption compared to wild-type females of corresponding age ($P < 0.001$, Student's two-tailed t -test). The difference in the number of embryos being resorbed in *SCP3*-deficient females at different ages was significant [$P < 0.05$, one-way analysis of variance (ANOVA) with fixed effects], whereas no significant difference in embryo resorption number were seen for wild-type females (one-way ANOVA with fixed effects). Data represent mean \pm SEM.

revealed that *SCP3*-deficient females contained an average of 2.6 resorbed embryos, whereas resorbed embryos were rarely observed in wild-type females (Fig. 1B). The reduced litter size in *SCP3*-deficient females is therefore due to embryo death in utero. Older (24-week-old) *SCP3*-deficient females showed a further reduction in offspring number (Fig. 1A). To see if this could be explained by increased embryo death in utero, the numbers of live and dead embryos in 12-, 16-, and 24-week-old females were compared (Fig. 1B). We found that older *SCP3*-deficient females contained more resorbed, and fewer live, embryos. We conclude that absence of *SCP3* affects embryo survival in an age-dependent manner.

We postulated that the embryo death observed in *SCP3*-deficient females could be due to generation of aneuploid oocytes resulting from chromosomal segregation errors.

Karyotypic status was monitored in one-cell zygotes, which contain discrete maternally and paternally derived pronuclei, enabling independent assessment of the respective karyotypes. Seven of 17 one-cell zygotes derived from *SCP3*-deficient females displayed chromosomal aberrations, compared with 0 of 90 one-cell zygotes from wild-type females (Fig. 2A). We propose that *SCP3* deficiency in oocytes during meiosis results in inherited aneuploidy leading to embryo death. Chromosomal abnormalities in one-cell zygotes from *SCP3*-deficient oocytes are likely caused by recombinational errors during meiosis. To find out when these errors occur, we first investigated metaphase I (MI) oocytes from wild-type and *SCP3*-deficient females (Fig. 2B). Forty-seven of 93 MI oocytes from 13- to 14-week-old mutant females contained univalents (i.e., homologs

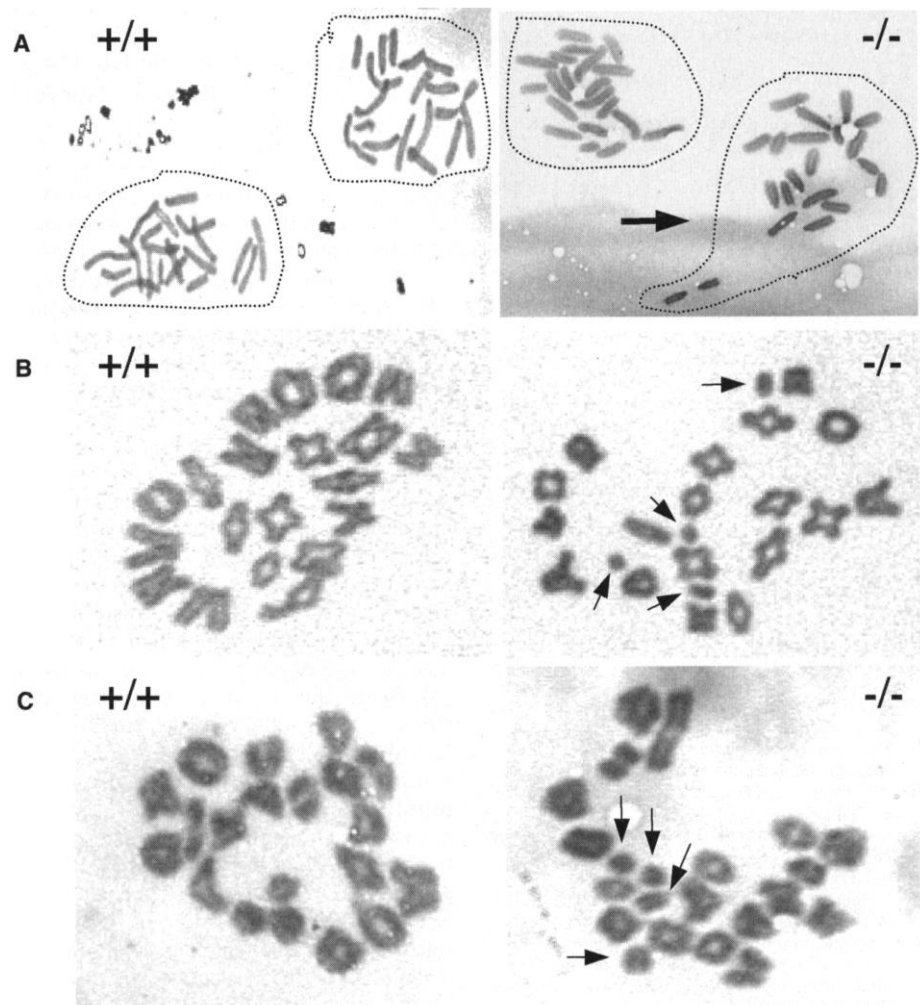


Fig. 2. One-cell zygotes and oocytes from *SCP3*-deficient females are chromosomally abnormal. 12- to 16-week-old wild-type or *SCP3*-deficient females were paired with wild-type males. Cells derived from wild-type females are indicated by +/+, whereas cells taken from *SCP3*-deficient females are indicated by -/-. **(A)** Zygotes at the one-cell stage were isolated and the mitotically arrested chromosomes karyotyped (13). The individual pronuclei are indicated by a dotted line; the arrow indicates a pronucleus with one extra chromosome (a total of 21 chromosomes). MI **(B)** or diakinesis **(C)** oocytes were analyzed for achiasmatic chromosomes (13). Arrows in **(B)** and **(C)** indicate univalent chromosomes.

REPORTS

not held together by chiasmata), whereas no univalents were found in 75 oocytes from wild-type females. Most of the affected MI oocytes contained one to three pairs of univalents (Fig. 2B). Furthermore, chiasmata distribution in 18 MI wild-type and 54 *SCP3*-deficient oocytes, indicated that the number of bivalents having a double exchange decreased two- to threefold in *SCP3*-deficient oocytes (0.6 ± 1.0 , SEM) compared to wild-type (1.6 ± 1.3 , SEM). These data show that chiasmata number is slightly reduced in *SCP3*-null oocytes. Because short chromosomes are held together by only one chiasma (10), they are at greater risk of being converted into univalents. Indeed, analysis of *SCP3*-null MI oocytes showed that a majority of the identified univalents are short chromosomes (Fig. 2B).

To define whether formation of univalent

chromosomes is due to a failure to establish or to maintain chiasmata during meiosis, we looked for achiasmatic homologs in oocytes at the diakinesis stage of meiosis. At this stage, the spindle has not yet become attached to the chromosomes, reducing the risk of losing preformed chiasmata. Approximately 50% of the *SCP3*-deficient diakinesis oocytes contained univalents, whereas virtually no univalents were observed in wild-type oocytes (Fig. 2C). This strongly suggests that the achiasmatic homologs formed in *SCP3*-deficient MI oocytes are due to a failure to establish chiasmata between homologous chromosomes.

Absence of *SCP3* thus appears to have a subtle but distinct effect on meiotic recombination. The recombination protein *DMC1* (11) forms similar arrays of foci in wild-type and *SCP3*^{-/-} zygotene oocytes (9), however, indi-

cating that early meiotic recombination activities were not substantially affected in mutant oocytes. Recombination in wild-type and *SCP3*-deficient pachytene oocytes was monitored, using the recombination protein *MLH1* (Fig. 3A), a marker for the chiasma structure (12). *MLH1* foci are formed in the absence of *SCP3* and the foci associate with synapsed meiotic chromosomes labeled by *SCP1*, a core component of the TF of the SC (2) (Fig. 3A). We observed a slight increase in the average number of *MLH1* foci associated with *SCP1* fibers in mutant oocytes (26.0 ± 1.5 , SEM) compared to wild-type cells (24.2 ± 0.8 , SEM), as well as a larger variability in foci number between individual mutant cells (9). Finally, we measured crossing-over frequency in offspring from *SCP3*^{-/-} and wild-type females, using polymorphic microsatellite markers. The F₂ offspring and their parents were typed using four pairs of polymorphic microsatellite markers on four separate chromosomes (Table 1). Despite a slight variability in the recombination rates for the different chromosomes analyzed, the crossing-over process is clearly active in mutant oocytes at about wild-type levels. We conclude that the recombination process in *SCP3*-null oocytes is functional and only subtly affected by the absence of *SCP3*.

Lack of *SCP3* could alter SC structure, thereby disturbing chiasma formation and chromosome segregation. *SCP1* formed linear filaments in *SCP3*-null pachytene oocytes. However, these filaments frequently contained axial gaps (Fig. 3A), in some cases separating the *SCP1* fiber from the terminally-located centromeric region of the chromosomes (9). These axial gaps suggest that short stretches of the homologs synapse incorrectly without *SCP3*. *SCP1* fiber length in *SCP3*-deficient pachytene oocytes increased twofold over the wild-type (Fig. 3B), indicating that chromatin compaction of the axial core is severely affected in the absence of *SCP3*. To monitor the effects of *SCP3* deficiency on SC formation, silver-stained wild-type and *SCP3*-deficient pachytene oocytes were compared. SC structures seen in wild-type oocytes were found to be absent in *SCP3*-deficient oocytes (13). Furthermore, immunofluorescence microscopy analysis of *SCP2* did not produce the expected filamentous signal in *SCP3*-deficient pachytene oocytes, instead forming nuclear foci, approximately half of which colocalized with a centromere marker (13). We found that *SCP3* is required for AE formation, *SCP2* integration into the AE, and uninterrupted *SCP1*-mediated synapsis.

Despite the prevalence of aneuploidy (1), very little is known about the causes of chromosomal nondisjunction in female germ cells. We show here, in a mouse model system, a direct link between *SCP3*-deficiency in females and the fate of their offspring. We demonstrate that a slight decrease in chiasma number leads to

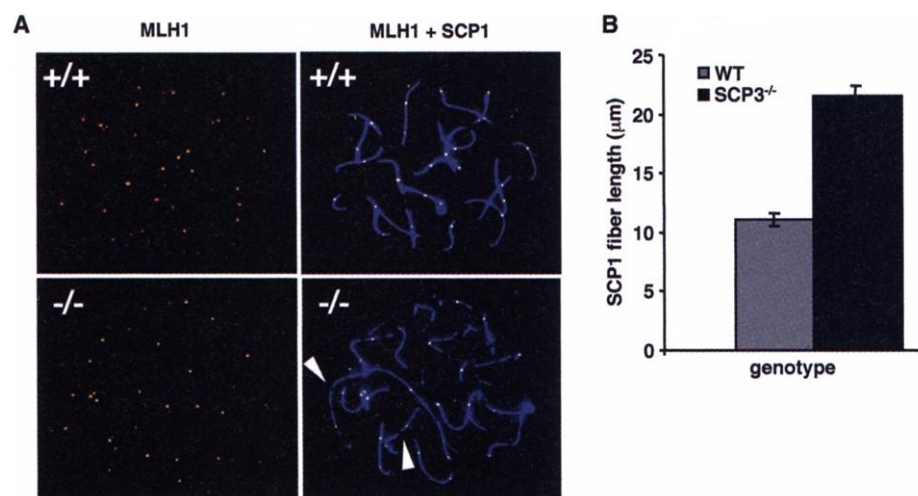


Fig. 3. Altered *MLH1* and *SCP1* expression in *SCP3*-deficient oocytes. Cells derived from wild-type females are indicated by +/+, whereas cells taken from *SCP3*-deficient females are indicated by -/-. (A) *SCP3*-deficient or wild-type oocytes were isolated, fixed and analyzed by immunofluorescence microscopy (13). The distribution of *MLH1* (red/white dots) and *SCP1* (blue fibers) are shown for pachytene oocytes. Arrowheads indicate axial interruptions of the *SCP1* fiber. Because of the axial interruptions seen in the *SCP1* fiber, it was not possible to determine with certainty whether some homologs completely lacked *MLH1* foci. (B) *SCP1* fiber length increases in *SCP3*-deficient oocytes. Total *SCP1* fiber length in 10 individual wild-type or *SCP3*-deficient pachytene oocytes was measured and average fiber length calculated. Data is presented as mean \pm SEM.

Table 1. Loss of *SCP3* in oocytes has a subtle, but distinct effect on crossing-over frequency. Backcrossed *SCP3*^{+/-} females (C57BL/6NCrIBR) were mated to *SCP3*^{+/-} males (C57BL/6NCrIBR \times 129/Ola) to generate F₁ hybrid mice (13). F₁ hybrid female mice nullizygous or wild type for *SCP3* were mated with wild-type males (C57BL/6NCrIBR) to generate F₂ offspring. Tail DNA from F₂ offspring and their parents was PCR typed using four pairs of polymorphic microsatellite markers for chromosomes 12, 15, 17, and 18. Crossing-over frequency was evaluated by χ^2 testing derived from the 2 \times 2 contingency test.

Chromosome	Genotype	Crossing-over events	Offspring number	Crossing-over frequency	Chi-square (probability)
12	<i>Scp3</i> ^{+/+}	19	57	33.3	16.2 (<0.0001)
	<i>Scp3</i> ^{-/-}	5	22	22.7	
15	<i>Scp3</i> ^{+/+}	11	55	20.0	2.7 (>0.05)
	<i>Scp3</i> ^{-/-}	10	40	25.0	
17	<i>Scp3</i> ^{+/+}	3	20	15.0	3.6 (>0.05)
	<i>Scp3</i> ^{-/-}	3	33	9.1	
18	<i>Scp3</i> ^{+/+}	13	43	30.2	6.0 (<0.02)
	<i>Scp3</i> ^{-/-}	15	29	51.7	

increased recombination failure for the smallest chromosomes and to a corresponding increase in aneuploid embryos in SCP3-null females.

What then is the role of SCP3 and how does its absence cause chromosomal nondisjunction? SCP3 expression is restricted to meiotic prophase I cells, disappearing during diakinesis in female oocytes (14). The structural changes seen in meiotic chromatin due to SCP3 absence strongly suggest that nondisjunction is caused by errors that initially occur at pachytene. It was also found that the SCP1 fiber in SCP3-deficient pachytene oocytes contained axial gaps, indicating incomplete homolog synapsis. Incorrect homolog alignment could affect the crossing-over process that generates chiasmata. SCP1 homologs in yeast (Zip1) and *Drosophila* [C(3)G] have been shown to be important for both synapsis and crossing-over, and their absence results in a high level of nondisjunction (15, 16). Mutations in these two proteins that introduce noncontiguous axial gaps in their respective TF structures reduce the levels of meiotic exchange and crossover interference. In addition, mutations in genes that affect crossover interference randomize crossover distribution between chromosomes, such that chromosomes may fail to cross over and therefore nondisjoin (2, 17, 18). The observed changes in chromatin structure and SCP1 organization along the homologs in SCP3-null oocytes could therefore affect crossover interference, affecting both chiasma positioning and frequency.

The increased embryo death in older SCP3^{-/-} females is notable. A reduced oocyte pool in humans has been proposed to result in a premature increase in aneuploidy and embryo death (19). By this model, a shortened reproductive life span, resulting from a substantial loss of oocytes in the developing SCP3^{-/-} ovary could explain the increased embryo death. Alternatively, SCP3 absence could have two effects on chromosomal nondisjunction, an early effect seen as a reduction in chiasmata number and a later effect that only manifests itself in older females. The second model could be explained as a two-hit mechanism, as previously suggested for aging human oocytes (20). The first hit would be due to a reduction in crossover interference resulting in suboptimal positioning of chiasmata along the chromosomes, whereas the second hit would occur due to an inability of older oocytes to resolve chiasmata located at certain chromosomal regions. The model system described here should thus be valuable toward understanding the basis for meiotic nondisjunction and age-dependent aneuploidy in human oocytes.

References and Notes

1. T. Hassold, P. Hunt, *Nature Rev. Genet.* **2**, 280 (2001).
 2. D. Zickler, N. Kleckner, *Annu. Rev. Genet.* **33**, 603 (1999).

3. K. Schmekel, B. Daneholt, *Trends Biochem. Sci.* **5**, 239 (1995).
 4. K. Nasmyth, *Annu. Rev. Genet.* **35**, 673 (2001).
 5. J. A. C. Schalk et al., *Chromosoma* **107**, 540 (1998).
 6. L. Yuan et al., *J. Cell Biol.* **142**, 331 (1998).
 7. J. Peltari et al., *Mol. Cell Biol.* **21**, 5667 (2001).
 8. L. Yuan et al., *Mol. Cell* **5**, 73 (2000).
 9. M. R. Hoja, J. G. Liu, L. Yuan, E. Brundell, C. Höög, data not shown.
 10. N. M. Lawrie, C. Tease, M. A. Hulten, *Chromosoma* **140**, 308 (1995).
 11. M. Tarsounas, T. Morita, R. E. Pearlman, P. B. Moens, *J. Cell Biol.* **147**, 207 (1999).
 12. L. K. Anderson, A. Reeves, L. M. Webb, T. Ashley, *Genetics* **151**, 1569 (1999).
 13. Supplementary figure and details of experimental procedures are available on Science Online at www.sciencemag.org/cgi/content/full/296/5570/1115/DC1
 14. C. A. Hodges, R. LeMaire-Adkins, P. A. Hunt, *J. Cell Sci.* **114**, 2417 (2001).
 15. K. S. Tung, G. S. Roeder, *Genetics* **149**, 817 (1998).
 16. S. L. Page, R. S. Hawley, *Genes Dev.* **15**, 3130 (2001).
 17. M. Sym, G. S. Roeder, *Cell* **79**, 283 (1994).
 18. D. P. Kaback, D. Barber, J. Mahon, J. Lamb, J. You, *Genetics* **152**, 1475 (1999).
 19. J. Kline, A. Kinney, B. Levin, D. Warburton, *Am. J. Hum. Genet.* **67**, 395 (2000).
 20. N. E. Lamb et al., *Nature Genet.* **14**, 400 (1996).
 21. Supported by the Swedish Cancer Society, The Swedish Research Council, Pharmacia Corporation, Petrus and Augusta Hedlunds Stiftelse, and Karolinska Institutet. We thank E. Brundell and M.-L. Spångberg for technical assistance, C. Heyting for antisera, and P. A. Hunt, J. Schimenti, K. Schmekel, M. Sjöberg, and B. Daneholt for helpful discussions.

6 February 2002; accepted 29 March 2002

Ablation of Insulin-Producing Neurons in Flies: Growth and Diabetic Phenotypes

Eric J. Rulifson,^{1,3*} Seung K. Kim,^{1,2} Roel Nusse^{1,3}

In the fruit fly *Drosophila*, four insulin genes are coexpressed in small clusters of cells [insulin-producing cells (IPCs)] in the brain. Here, we show that ablation of these IPCs causes developmental delay, growth retardation, and elevated carbohydrate levels in larval hemolymph. All of the defects were reversed by ectopic expression of a *Drosophila* insulin transgene. On the basis of these functional data and the observation that IPCs release insulin into the circulatory system, we conclude that brain IPCs are the main systemic supply of insulin during larval growth. We propose that IPCs and pancreatic islet β cells are functionally analogous and may have evolved from a common ancestral insulin-producing neuron. Interestingly, the phenotype of flies lacking IPCs includes certain features of diabetes mellitus.

The *Drosophila* genome contains five *Drosophila* insulinlike peptide genes (*dilp1* through *-5*) with significant homology to mouse and human insulins and two others with far less similarity (*dilp6* and *-7*). These genes are expressed in tissues ranging from early embryonic mesoderm to small clusters of larval brain neurons, ventral nerve cord neurons, salivary gland, and midgut (1). Using messenger RNA (mRNA) in situ hybridization, we established that the most prominent insulin gene expression during larval stages, a period of intensive feeding and rapid growth, is within two bilaterally symmetric clusters of neurosecretory cells in the pars intercerebralis region of the protocerebrum (fig. S1).

An 859-base pair promoter fragment, comprised of sequences immediately 5' of *dilp2*, was sufficient to drive gene expression in the small clusters of larval brain neurons

that express *dilp1*, *-2*, *-3*, and *-5* (fig. S1). To assess the role of the brain IPCs as an insulin-producing endocrine system, we ablated the brain IPCs using the *dilp2* promoter to express the cell death-promoting factor, Reaper (2). The IPC ablation results in deficiency of brain neuron-derived insulin only (fig. S2). IPC ablation caused undergrowth phenotypes, developmental delays, and lethality similar to *Drosophila* insulin receptor (DInR) mutants (1, 3). To rule out an underlying cause of these phenotypes other than insulin deficiency, such as non-IPC death from Reaper or loss of other essential brain IPC functions, we used a heat shock-inducible *dilp2* transgene with ubiquitous expression to reverse the effect of the IPC ablation.

We quantified the defect in growth by comparing larval length after 120 hours of development, a time at which synchronized cultures of normal larvae will reach wandering third instar and puparium formation. [Larval phenotypes are shown in (fig. S3).] After IPC ablation, larvae attained a mean length only 58% of normal size (Fig. 1A, center). Larvae with IPCs ablated but expressing the inducible *dilp2* transgene had

¹Department of Developmental Biology, ²Department of Medicine (Oncology Division), ³Howard Hughes Medical Institute, Beckman Center B300, Stanford University, Stanford, CA 94305-5329, USA.

*To whom correspondence should be addressed. E-mail: rulifson@cmgm.stanford.edu